

Corrosion Behavior of Aluminum Alloy 6061 with Grain Refiner Al-6Ti in Salt Solution (3.5% NaCl) After Heat Treatment.

Eltohamy R. Elsharkawy

Nuclear & Radiological Regulatory Authority, Quality Control and Quality Assurance Depart. Cairo, Egypt

ABSTRACT

Aluminium and its alloys are the most used nonferrous metals because of their satisfactory properties. Especially the corrosion resistant in different mediums is the most important reason for this. Aluminum alloy 6061 have been employed as structural material for water-cooled nuclear reactors as a cladding material for the fuel elements on an Egyptian experimental reactor (MTR – type). The aim of this work is to study the effect of grain refiner Al-6Ti on the electrochemical and corrosion behavior of aluminum alloy 6061 (AA6061) nuclear grade because the good corrosion resistance against coolant water is very important for nuclear fuel cladding material. This is done by investigating the effect of addition 4gm/kg amount of grain refiner Al-6Ti to AA6061 on corrosion behavior. The corrosion behavior was investigated by measuring linear polarization, it can be noticed from the polarization curves show a regular pattern and the cathodic current densities decreases with the grain refiner. The best working conditions for Al-6Ti master alloy being used as grain refiner in aluminium alloy 6061 were 4 gm/kg of refiner quantity, 720°C casting temperature and 10 minutes holding time for grain refiner prior casting to give the best corrosion resistance after artificial aging at 8 hour at 180°C.

Date of Submission: 22 December 2016



Date of Accepted: 05 January 2017

I. INTRODUCTION

The AA6061 has good nuclear properties, such as small cross section for neutron absorption, good corrosion resistance against coolant water, toughness even after long term exposure in a neutron field, and short life - times of the radioactive nuclei produced by nuclear reactions. Recently, high neutron flux reactors have been developed and the core materials are required to achieve better resistance against neutron flux exceeding the 10^{15} n/cm^2 value [1]. Materials are required to achieve better resistance against neutron flux exceeding the 10^{15} n/cm^2 value [1]. Grain refining is widely practiced in the commercial production of virtually all aluminium alloys, whether wrought or cast [2, 3]. Equiaxed grain structure ensured uniform mechanical properties, reduced chemical segregation, porosity and hot tearing and increased pressure tightness; the advantages during the subsequent processing stages are improved mechanical properties in heavier sections, consistent properties after heat treatment, improved machinability and better appearance in anodized coatings in ingot. Reduction in grain size can be achieved in three different stages - during solidification of the molten metal, thermomechanical treatments involving recovery and recrystallization of the deformed material and severe plastic deformation using processes such as, a hydrostatic extrusion and roll bonding [4-5].

The most common method of achieving grain refinement in aluminium is the use of specific nucleating addition - salts or master alloys. Grain refining agents such as titanium or boron are added singly or in combination to aluminium melts in very small quantities that do not alter the base composition of the melt to any great degree. These additions have historically been made as master alloys (hardeners) with aluminium in the form of shot, waffles, or briquettes [6]. The methods favoring the formation of fine grains include addition of trace elements in the form of master alloys, inoculation of borides and carbides, use of ultrasonic treatment or electromagnetic field. Inoculation is the most commonly employed method and is carried out using grain refiners such as Al-6Ti master alloy. When aluminum surfaces are exposed to the atmosphere, a thin invisible, strongly adherent oxide film forms immediately which protects the metal from further oxidation. This film gives aluminum and its alloys their high resistance to corrosion. Protection by this film is limited to environments in which it is stable or only slightly soluble. According to Pourbaix diagram, passivity of aluminum is limited to the pH range from about 4 to 9. Above and below this range, aluminum and its alloys normally exhibit uniform corrosion attack. However, in the pH range where the oxide film is stable, the protective effect of the film is greatly influenced by its integrity. Any defects or discontinuities in the passive film will expose the underlying metal to the surrounding corrosive medium and will lead to the onset of localized corrosion [7-8]. The aim of this work is to assess the influence of aging and grain refiner of the AA6061 on its corrosion and passive film properties.

II. EXPERIMENTAL WORK

2.1 Material and Methods

Aluminum alloy 6061 with chemical composition as shown in Table (1) is used in the present study. The received alloy form is an extruded plates 11 mm thickness at the case T₀ heat

Table. 1 Chemical Composition of A6061 Aluminum alloy (wt %)

Si %	Fe %	Cu %	Mn %	Mg %	Cr %	B %	Ti %	Others %	Al
0.53	0.16	0.31	0.01	0.93	0.05	0.0007	0.01	0.01	Balance

treatment e.g. annealed material. Aluminum alloy 6061 was melted in an electrical resistance furnace in a crucible of a 200 gm of aluminum alloy 6061 capacity. The best working conditions for Al-6Ti master alloy being used as grain refiner in aluminium alloy 6061 were 4gm/kg of refiner quantity, 720°C casting temperature and 10 minutes holding time for grain refiner prior casting. The typical chemical composition of the used grain refiners are depicted in Table. 2.

Table.2 Chemical Analysis of the grain refiners Al-6Ti (wt. %)

Grain refiner	Ti (%)	B (%)	C (%)	Fe (%)	Si (%)	Al
Al- 6Ti	6	-	-	0.10	0.02	Balance

2.2. Heat Treatment

About 200 g of the matrix alloy 6061 was melted in an electrical resistance furnace of 8 kW power in an aluminium oxide crucible. The melting operation was performed. Once the melt reached 720°C, it was degassed for 2 minutes with argon gas at a flow rate of 0.5 liters per minute. The grain refiners were added at different addition level 4 g/kg . The melts were stirred manually with a graphite rod to distribute the master alloys uniformly in the melts. The temperature of the melt was measured by using a Ni-CrNi thermocouple and the melt temperature was monitored to ensure a fixed casting temperature. Various factors such as casting temperature, holding time for the grain refiner in molten AA 6061 are taken into consideration to obtain the best operating conditions for grain refinement of the wrought aluminium alloy 6061. The melt is then casted into steel mold of 40 mm diameter and 50 mm in length and naturally cooled down to room temperature. These castings were sectioned at a height of 20 mm from the bottom, polished and etched with 1% HF to reveal the grain boundaries. The average grain size was measured using a line intercept method (ASTM E112-96) and with quantitative microscopic analysis. The samples were examined under optical microscope and scanning electron microscope (SEM) DSM 950. The samples were heat treated precipitation solution at 550°C for 1 hour and artificial aging for 0, 4, 8 and 16 h at 180°C.

2.3 Electrochemical Corrosion testing

Prior to corrosion behavior studies, the samples were ground on SiC grinding papers from 240 till 1000 grade, followed by polishing on polishing lapped cloth using 1µm diamond suspension. Then the polished samples were degreased with ethanol before immersion in the test solution. The electrochemical corrosion behavior of the samples was studied by applying the potentiodynamic polarization technique using a potentiostat (Electrochemical Impedance Analyzer, Model 6310) interfaced to a computer and a three-electrode cell with the sample as a working electrode of exposed area 100 mm², a saturated calomel reference electrode (SCE)

2.4. SEM and Optical microscopy, grain size measurement

The etched specimens were tested one by one using an optical microscope. The photographs of the microstructure were taken with help of a Camera fitted with a microscope. The average grain size was measured using a line intercept method (ASTM E112-96) and with quantitative microscopic analysis. The samples were examined under optical microscope and scanning electron microscope (SEM) DSM 950.

III. RESULTS AND DISCUSSION

3.1 Microstructure Characterization before Corrosion

A characterization study of the grain refiners in use was carried out to identify the present phases since manufacturer only gave chemical compositions. X-ray diffraction “XRD” and “EDX” analysis were used. The binary grain refiner (Al-6Ti) was thoroughly examined for microstructure and the present phases. Figure 1 shows the microstructure of Al-6Ti binary master alloy, it is clear from this figure that the present phases form petal-like shapes in addition to some plates-like shapes. X-ray diffraction studies were performed on the Al-6Ti binary master alloy in order to identify the phases present (figure 2. a). Figure 2.b clearly shows number of

identifiable phases. Based on Figure 3 representing phase diagram of Aluminum – titanium system, it's expected that during cooling to room temperature that α -Al and Ti Al₃ will form stably [3].

To confirm the phase diagram expectations an EDX examination was undertaken. Figure (2b) shows the TiAl₃ phase as expected.

When one considers the Al-Ti phase diagram (figure3), it is clear that master alloy containing 0.6%Ti will be primarily a mixture of α -Al and crystalline TiAl₃. It is found that Ti Al₃ can assume three different shapes depending on the temperature history of the master alloy. Rapid cooling of saturated solution from high temperature forms petal-like shapes, slow cooling from high temperature produces plates, and chemical reactions at low temperature produce “blocky” Ti Al₃ crystal. [9]. Also, it is found that the grain refining response of the alloy depends on the morphology of the titanium aluminide [10]. Blocky crystals tend to act fast, but their effect fades quickly. Petal and plate-like structures act more slowly, but their grain refining efficiency improves with time and lasts longer [3].

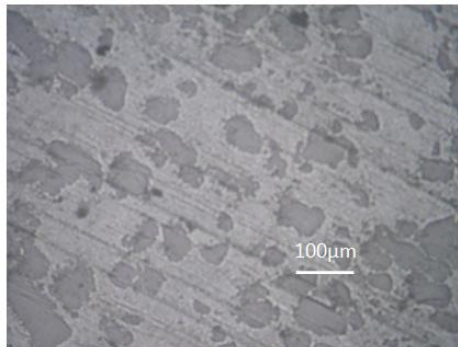


Figure 1 shows the microstructure of Al-6Ti binary master alloy[3]

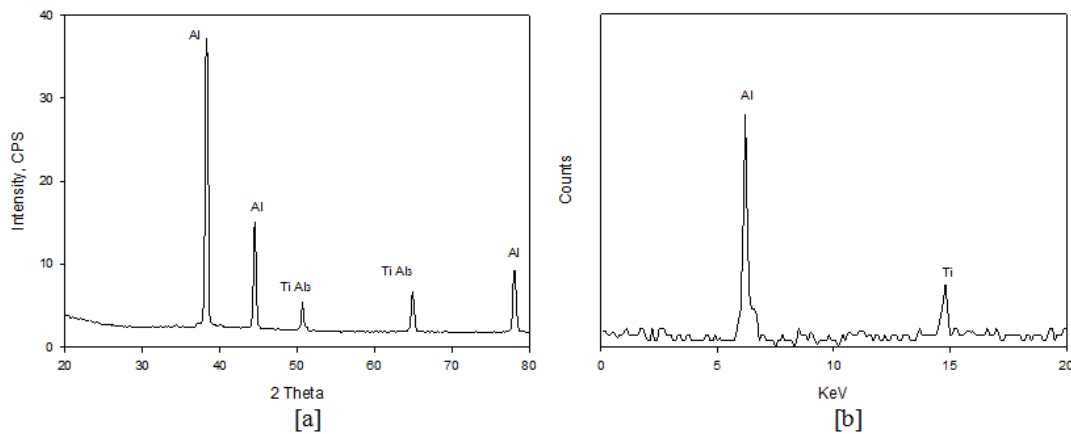


Figure .2.a. X-Ray diffraction of Al-6Ti binary master alloy, and 2.b, The EDX of Al₃Ti master alloy [3].

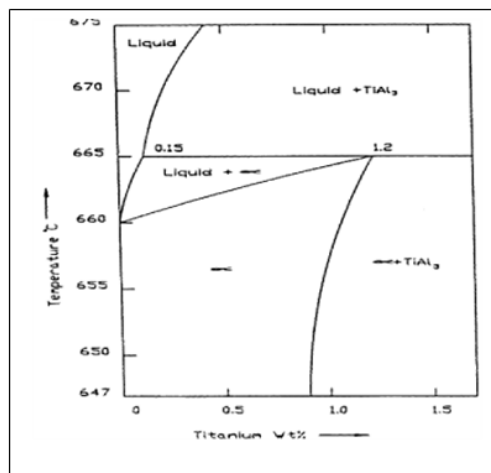


Figure .3Aluminum-titanium system phase diagram [3]

Figure.4 a- b show the microstructure of AA6061 without grain refiner a, as received and b, after peak aging . For figure 4. C-d show the microstructure of AA6061 with grain refiner Al-6Ti C, as received after casting and d, after peak aging . It is clear from Fig. 4c,d the effect of grain refiner Al- 6Ti with AA6061 the grain size after the addition of grain refiner reached 64 μm as casting and after aging 12 μm .

For Al-Ti master alloys contain numerous titanium aluminide crystals. When these are added to aluminum alloy 6061, they act both to nucleate solid grains and to slow the initial growth rate of solid after nucleation. The resulting increased ratio of nucleation rate to growth rate gives a fine -grained ; when titanium is added at concentrations less than the hyperperitectic solubility of TiAl₃ (0.15 % Ti at 665°C), the grain-refining effect time of the master alloy fades with time as the TiAl₃ crystals dissolve. The increase in fine grain size could be attributed to the size, size distribution and change in morphology of aluminide particles present in the master alloys. On the other hand, when Al-Ti is the grain refiner, it is the Al₃Ti phase acts as the nucleant and the presence of Si or Mg improves its nucleation potential.

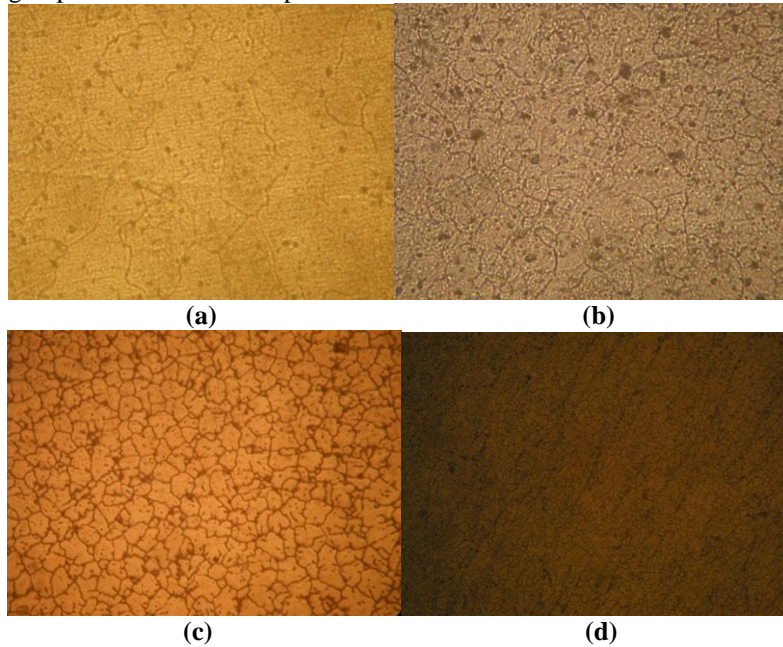
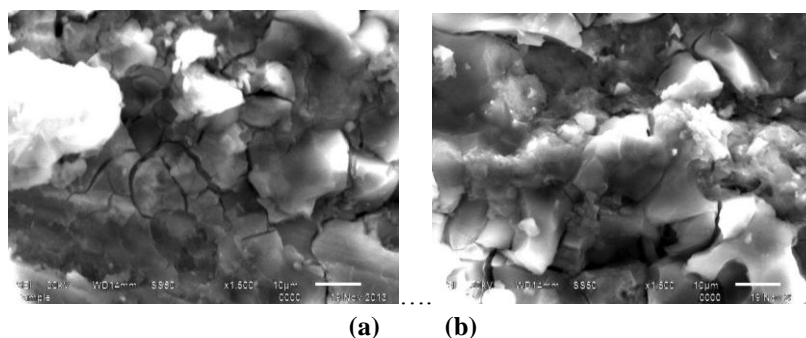


Figure.4 a- b show the microstructure of AA6061 without grain refiner a, as received and b, after peak aging, for figure 4. C-d show the microstructure of AA6061 with grain refiner Al-6Ti C, as received after casting and d, after peak aging.

3.2. Metallographic studies of the AA6061 with Al-6Ti grain refiner after corrosion

Figure 5 shows the views of the AA6061 with grain refiner Al- 6Ti samples, taken by scanning electron microscope (SEM) after they were kept inside 3.5% NaCl for 120 hours. The TiAl₃ intermetallic phase regions behave as cathode and the near α - Al phase behaves anodically and dissolves. By the Ti content 6 % the average area ratio of the intermetallic phases increases [12]. So with increasing aging time the size of the local cathode areas increases and this leads more dissolution of the Al matrix. Figure 5.c shows the SEM images of samples as received (a) , aging time 4hr (b), aging time 8hr (peak aging , c) and aging time 16 hr (d) . It can be seen that corrosion resistance in case (c) is more severe than in the another cases. The variation of the grain size number with the change of the aging time, it is clearly seen from Fig. 5 that the grain size is bigger for the as received sample and gets finer with samples at peak aging 8hr.



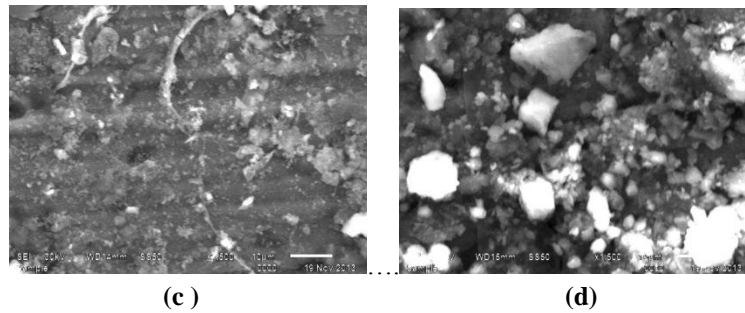


Figure. 5 shows the images of AA6061 with grain refiner Al- 6Ti samples, taken by scanning electron microscope (SEM) after (a) as received, (b) aging time ,(4h) (c) peak aging (8h), and (d) aging time (16h) (the magnifications for all specimens were 1500 X).

3.3 Potentiodynamic polarization measurement

Corrosion behavior of Al alloy 6061 with grain refiner Al-6Ti after solution treatment and different aging time (0 , 4, 8 and 16 hr) at temperature 180 °C were determined through potentiodynamic polarization method in the solutions of potentiodynamic polarization curves of the alloys in the solutions of 3.5% NaCl are seen on Figs. 6 to 9, respectively. Table 3 shows the values of I_{corr} and E_{corr} obtained from these curves. According to this, increase in aging time in Al alloy 6061 with grain refiner Al-6Ti cause changes in corrosion potential. Corrosion potential inside 3.5% NaCl ranged between -715 mV and -757 mV, corrosion current density inside 3.5% NaCl ranged between $1.21 \mu A/cm^2$ and $2.07 \mu A/cm^2$. In case of aging time 8h, corrosion current density decreased compared with the another aging times.

Table 3. Kinetic parameters of AA6061 with grain refiner Al-6Ti in 3.5% NaCl medium at different aging time.

Aging time	β_a (mVdec ⁻¹)	β_c (mVdec ⁻¹)	I_{corr} ($\mu A/cm^2$)	E_{corr} (mV)	mmy
0	178	292	2.07	-757	0.045
4	137	305	1.56	-749	0.037
8	123	319	1.21	-715	0.024
16	130	297	1.39	-724	0.032

The reason for much more significant increase in corrosion current density in the experiments done inside 3.5% NaCl solution is the active Cl⁻ ions existing in the solution. The effect of Cl⁻ ions decomposing the oxide layer formed on the surface accelerates corrosion and increases corrosion current density with increasing aging time more 8h. TiAl3 intermetallic phase formed inside the metal as a result of titanium addition into these alloys constructs cathode regions of the less localized cell inside the aluminium matrix. The main reason for that TiAl3 phase behaves as cathode is that the oxide film on this phase is thinner than that on the aluminium matrix because it is less inert and it constructs the regions in which electrons flowing resistance gets more. Beginning and spreading of hollow corrosion namely anodic dissolutions are seen in the aluminium matrix surrounding these phases after peak aging (16hr) [13].

Figure. 10 show the relation between aging time and corrosion rate per year, It is clearly seen from Fig. 10 that the increasing the aging time in the underaged region decreases the corrosion rate until time 8hr(peak aging) , after that the corrosion rate increase at aging time 16hr. This will increase the cathodic area fraction on the specimen surface at peak aging and consequently the cathodic reaction rate will be decreased. After peak aging (16hr), the anodic reaction will be derived at a higher rate giving increasing I_{corr} values with aging time(16hr) in the underaged region, it is expected that other fresh cathodic particles are more rapidly [14].

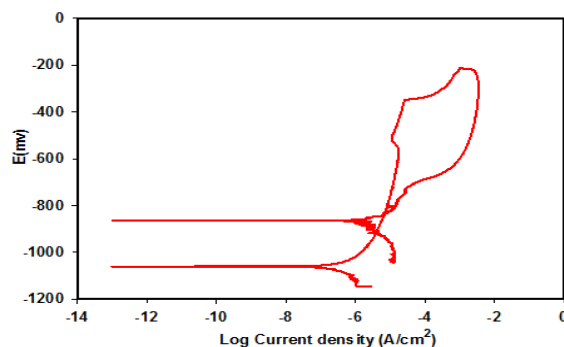


Fig.6 Anodic and cathodic polarization curve of AA6061 with Al-6Ti at aging time 0 hr in 3.5wt.% NaCl solution.

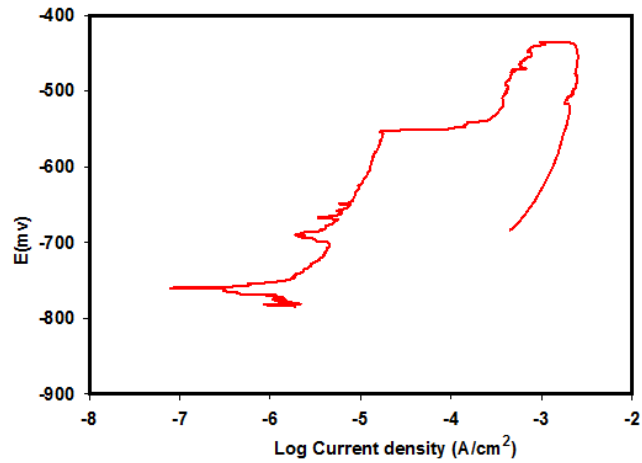


Fig.7 Anodic and cathodic polarization curve of AA6061 with Al-6Ti at aging time 4 hr in 3.5wt.% NaCl solution.

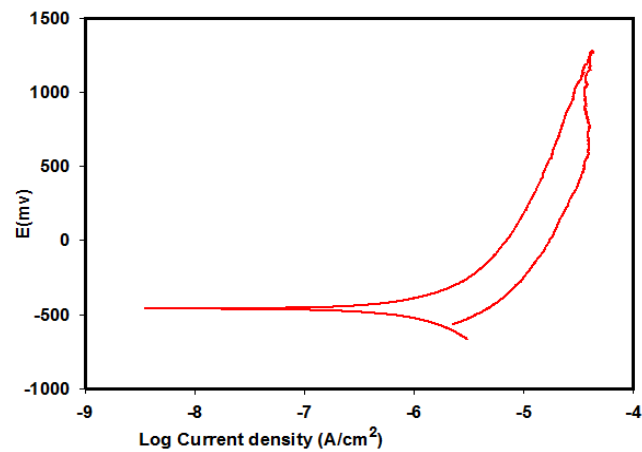


Fig.8 Anodic and cathodic polarization curve of AA6061 with Al-6Ti at aging time 8 hr in 3.5wt.% NaCl solution.

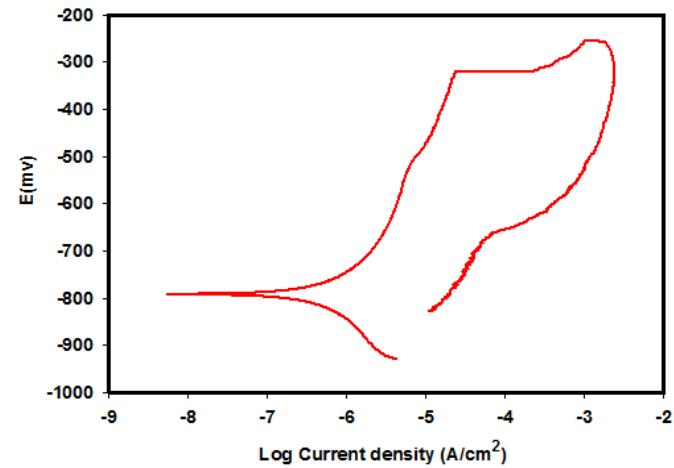


Fig.9 Anodic and cathodic polarization curve of AA6061 with Al-6Ti at aging time 16 hr in 3.5wt.% NaCl solution.

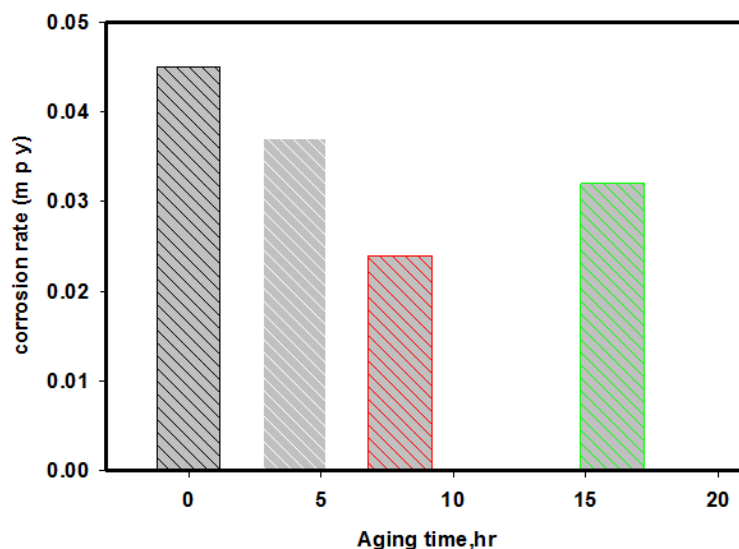


Fig 10. Relation between aging time(hr) and corrosion rate(m p y)

IV. CONCLUSION

The effect of grain refiner Al-6Ti on the electrochemical and corrosion behavior of aluminum alloy 6061 (AA6061) nuclear grade was studied by electrochemical method in 3.5 NaCl % solution with different PH values, corrosion rate decreased with the increase in aging time in all solutions until peak aging 8hr. However, the highest values of corrosion rate were in 0 aging time (as received). The changes in E_{corr} values exhibit different trends in the two test solutions. The E_{corr} values were shifted in the more noble direction in the NaCl solution for all aging conditions. The magnitude of the shift increased with the aging time in the underaged region to the peak condition and decreased again for the overaged samples. Titanium addition with grain refiner Al-6Ti to AA6061 causes intermetallic phase separation in the composition of TiAl₃. These TiAl₃ intermetallic phases construct local cathode regions inside the material and cause dissolutions at matrix regions close to them, therefore, increase in titanium amount in the material leads to the increase in local cathode areas and this caused increase in corrosion current density. It is known that, titanium intermetallic phases existing in the Al alloys have different morphologies. More comprehensive studies are required to determine the effects of these different morphologies on corrosion behaviour of alloys.

REFERENCES

- [1]. The aluminum association, Inc., Aluminum Now, Vol. 6, No. 3, 2004.
- [2]. M. K. Abbass, E. K. I Brahim, and E. S. Noem, "Effect of heat treatments on the mechanical properties and wear resistance of Al alloy matrix composite," J. of Engineering and Technology, University of Technology, Baghdad, vol. 29, no.12, 2011, pp. 518-533.
- [3]. E. Elsharkawy, et al. "Effect of the Al-6Ti and Al-4B grain refiner on the Microstructure and mechanical behavior of aluminium alloy 6061" Al-Azhar University Engineering Journal, JAUES Vol. 5, 2010. pp. 67-74.
- [4]. Mohammed. A. Amin, Influence of the Alloying Elements on Uniform and Pitting Corrosion Events Induced by SCN⁻ Anions on Al-6061 and Al-Cu Alloys Surfaces, (2010, Jordan Journal of Chemistry Vol. 6 No.1, 2011, pp. 91-105.
- [5]. Solhan Yhya, Afidah Abdul Rahim, Affaizza Mohd Shah, Ohana Adnan, Inhibitive Behavior of Corrosion of Aluminium Alloy in NaCl by Mangrove Tannin, Sains Malaysiana, 40(9)2011, pp. 953-957.
- [6]. El-Sayed M. Sherif, J.H. Potgieter, J.D. Comins, L. Cornish, P.A. Olubambi, C.N. Machio, Corros. Sci., 51, 2009, p. 1364.
- [7]. Emamy M, Daman AR, Taghiabadi R, Mahmudi M. Effects of Zr, Ti and B on structure and tensile properties of Al-10Mg alloy (A350). Int J Cast Metals Res 2004, pp. 11-17.
- [8]. H. Li; Z. Jiang; Q. Ma; Z. Li. Advanced Materials Research, 1180, 2011, pp. 217-218.
- [9]. J. Kubasek, D. Vojtech, Nonferrous Met. Soc. 23, 2013, pp. 1215-1225.
- [10]. M.R.S. Campos, C. Blawert K. U. Kainer, Mater. Sci. Forum 765, 2013, pp. 673-677.
- [11]. C. Li, Q. Pan, Y. Shi, Y. Wang, B. Li, Materials and Design 55, 2014, pp. 551-559
- [12]. Johnsson M, Sigworth GK. Study of mechanism of grain refinement of aluminium after addition of Ti- and B-containing master alloys. Metall Trans A, 1993, pp. 481-91.
- [13]. Easton MA, Stjohn DH. A model of grain refinement incorporating alloy constitution and potency of heterogeneous nucleant particles. Acta Mater, 2001, pp. 67-78.
- [14]. N. R. P. Swamy, and T. Chandrashekar, "Effect of heat treatment on strength and abrasive wear behavior of Al 6061-SiCp composites," Bull. Mater. Sci., vol. 33, no. 1, 2010, pp. 49-54.